International Journal of Fracture 77: 161–174, 1996.

Fracture mechanics analysis of cracked 2-D anisotropic media with a new formulation of the boundary element method

E. PAN and B. AMADEI
University of Colorado, Department of Civil Engineering, Boulder, CO 80309-0428, USA

Received 1 August 1995; accepted in revised form 5 January 1996

Abstract. A new formulation of the boundary element method (BEM) is proposed in this paper to calculate stress intensity factors for cracked 2-D anisotropic materials. The most outstanding feature of this new approach is that the displacement and traction integral equations are collocated on the outside boundary of the problem (no-crack boundary) *only* and on one side of the crack surfaces *only*, respectively. Since the new BEM formulation uses displacements or tractions as unknowns on the outside boundary and displacement differences as unknowns on the crack surfaces, the formulation combines the best attributes of the traditional displacement BEM as well as the displacement discontinuity method (DDM). Compared with the recently proposed dual BEM, the present approach doesn't require *dual* elements and nodes on the crack surfaces, and further, it can be used for *anisotropic media* with cracks of any geometric shapes. Numerical examples of calculation of stress intensity factors were conducted, and excellent agreement with previously published results was obtained. The authors believe that the new BEM formulation presented in this paper will provide an alternative and yet efficient numerical technique for the study of cracked 2-D anisotropic media, and for the simulation of quasi-static crack propagation.

1. Introduction

The boundary element method (BEM) has emerged as a powerful numerical method which has certain advantages over the finite element method. The BEM is particularly suited to cases where better accuracy is required due to problems such as stress concentrations or where the domain of interest extends to infinity. The most important feature of the BEM is that it only requires discretization of the boundary rather than the domain.

Stress intensity factors are important in the analysis of cracked materials. They are directly related to fracture propagation criteria. The singularity of stresses near a crack tip is a challenge to numerical modeling methods, even to the BEM. Previously, several methods within the scope of the BEM have been suggested for handling stress singularities: The first one is the Green's function method [1]. This method has the advantage of avoiding crack surface modeling and also gives excellent accuracy; it is, however, restricted to very simple crack geometries for which analytical Green's functions are available. The second one is the subregional method [2, 3]. The advantage of this approach is its ability to model cracks with any geometric shape. The disadvantage is an artificial subdivision of the original region into several subregions, thus resulting in a large system of equations. The third approach is the displacement discontinuity method (DDM) [4]. Instead of using the Green's displacements and stresses from point forces, the DDM uses Green's functions caused by point dislocations or point displacement discontinuities. This method is very efficient for crack problems in infinite domains where there is no no-crack boundary. Unfortunately, it is not suitable for finite domain problems, since the kernel functions in DDM involve singularities with order higher than those in the traditional displacement BEM.

SHIRLEY. INTERPRINT: PIPS Nr.:108689 ENGI
frac3396.tex; 26/06/1996; 11:58; v.5; p.1

In recent years, the dual BEM [5–8] has been proposed for the study of cracked media. Compared with the aforementioned first two methods, the dual BEM does not require the artificial subdivision of the region or the Green's functions corresponding to the crack. Compared with the DDM, the dual BEM can be used to solve finite domain problems with high order singularities on the crack surface *only*. To the authors' knowledge, however, the dual BEM has been applied *only* to isotropic elasticity problems [7, 9, 10]. Also, in the dual BEM, elements and nodes are collocated on both sides of the crack surface, which then *doubles* the number of the resulting algebraic equations along the crack.

In this paper, the authors proposed a new BEM formulation to calculate stress intensity factors in cracked 2-D anisotropic materials. The new formulation is an extension of the dual BEM and is such that the displacement integral equation is collocated on the outside boundary *only* and the traction integral equation on one side of the crack surface *only*. No double elements and nodes are required along the crack surface as compared to the dual BEM. The new BEM formulation thus possesses the best attributes of both the traditional displacement BEM and the DDM. Further, the hyper-singularity in the traction integral equation is handled by introducing a new Gauss quadrature formulae which is very similar to the traditional weighted Gauss quadrature but with a different weight. This new Gauss quadrature formulae is very accurate, and can be used for any curved crack geometry as compared to the piecewise straight crack geometry requirement for the dual BEM. For mixed mode problems, the decoupling technique developed by Sollero and Aliabadi [2] is employed to avoid the hyper-singular integral along the crack surface. The authors have also introduced a new set of crack tip elements which can dramatically improve the accuracy of the numerical calculation. Examples of calculation of stress intensity factors in infinite and finite anisotropic domains have shown that the proposed new formulation is simple, accurate, and yet easily applicable to complex crack geometry shapes.

2. Green's functions for 2-D anisotropic elasticity

The complex variable function method has been found to be very suitable for the study of 2-D anisotropic elastic media [11]. The Green's functions for point sources in these media have been studied by several authors, notably by Eshelby, Read and Shockley [12], Stroh [13] and Lekhnitskii [11]. In the following, we present briefly the Green's function solutions for point forces in a 2-D infinite and anisotropic medium. The procedure is similar to the one used by Lekhnitskii [11], Suo [14] and Pan and Amadei [15].

With three complex analytical functions $f_i(z_i)$, one can, in general, express displacements and stresses by

$$\begin{aligned} u_i &= 2\,\mathrm{Re}\left[\sum_{j=1}^{3} A_{ij} f_j(z_j)\right], \\ \sigma_{2i} &= 2\,\mathrm{Re}\left[\sum_{j=1}^{3} L_{ij} f_j'(z_j)\right], \\ \sigma_{1i} &= -2\,\mathrm{Re}\left[\sum_{j=1}^{3} L_{ij}\mu_j f_j'(z_j)\right]. \end{aligned} \tag{1}$$

In these equations, $z_j = x + \mu_j y$; Re denotes the real part of a complex variable or function; and $\mu_j (j = 1, 2, 3)$ are three distinct complex roots with positive imaginary part of the following equation:

$$l_4(\mu) l_2(\mu) - l_3^2(\mu) = 0, \tag{2}$$

where

$$\begin{aligned} l_2(\mu) &= \beta_{55}\mu^2 - 2\beta_{45}\mu + \beta_{44}, \\ l_3(\mu) &= \beta_{15}\mu^3 - (\beta_{14} + \beta_{56})\mu^2 + (\beta_{25} + \beta_{46})\mu - \beta_{24}, \\ l_4(\mu) &= \beta_{11}\mu^4 - 2\beta_{16}\mu^3 + (2\beta_{12} + \beta_{66})\mu^2 - 2\beta_{26}\mu + \beta_{22}. \end{aligned} \tag{3}$$

In (3),

$$\beta_{ij} = a_{ij} - \frac{a_{i3}a_{j3}}{a_{33}}, \tag{4}$$

for generalized plan strain problems, and

$$\beta_{ij} = a_{ij} \tag{5}$$

for plane stress problems (of monoclinic materials with the symmetry plane at $x_3 = 0$). In these two equations, a_{ij} are the elements of the compliance matrix.

Also in (1), the elements of matrix [**L**] are

$$\begin{bmatrix} -\mu_1 & -\mu_2 & -\mu_3\lambda_3 \\ 1 & 1 & \lambda_3 \\ -\lambda_1 & -\lambda_2 & -1 \end{bmatrix} \tag{6}$$

and the elements of the matrix [**A**] are

$$\begin{aligned} A_{1\alpha} &= \beta_{11}\mu_\alpha^2 + \beta_{12} - \beta_{16}\mu_\alpha + \lambda_\alpha(\beta_{15}\mu_\alpha - \beta_{14}), \\ A_{2\alpha} &= \beta_{21}\mu_\alpha + \beta_{22}/\mu_\alpha - \beta_{26} + \lambda_\alpha(\beta_{25} - \beta_{24}/\mu_\alpha) \qquad \alpha = 1, 2, \\ A_{3\alpha} &= \beta_{41}\mu_\alpha + \beta_{42}/\mu_\alpha - \beta_{46} + \lambda_\alpha(\beta_{45} - \beta_{44}/\mu_\alpha), \\ A_{13} &= \lambda_3(\beta_{11}\mu_3^2 + \beta_{12} - \beta_{16}\mu_3) + \beta_{15}\mu_3 - \beta_{14}, \\ A_{23} &= \lambda_3(\beta_{21}\mu_3 + \beta_{22}/\mu_3 - \beta_{26}) + \beta_{25} - \beta_{24}/\mu_3, \\ A_{33} &= \lambda_3(\beta_{41}\mu_3 + \beta_{42}/\mu_3 - \beta_{46}) + \beta_{45} - \beta_{44}/\mu_3. \end{aligned} \tag{7}$$

In (6) and (7),

$$\lambda_1 = -\frac{l_3(\mu_1)}{l_2(\mu_1)}; \qquad \lambda_2 = -\frac{l_3(\mu_2)}{l_2(\mu_2)}; \qquad \lambda_3 = -\frac{l_3(\mu_3)}{l_4(\mu_3)}. \tag{8}$$

For concentrated forces acting at the source point (x^0, y^0), the complex functions in (1) can be expressed as [14]

$$f_j(z_j) = \sum_{k=1}^{3} \frac{-1}{2\pi} D_{jk} P_k \ln(z_j - z_j^0), \tag{9}$$

where $z_j^0 = x^0 + \mu_j y^0$, $P_k (k = 1, 2, 3)$ is the magnitude of the point force in the k-direction; and

$$\begin{aligned} \boldsymbol{D} &= \boldsymbol{A}^{-1}(\boldsymbol{B}^{-1} + \bar{\boldsymbol{B}}^{-1})^{-1}, \\ \boldsymbol{B} &= i\,\boldsymbol{A}\boldsymbol{L}^{-1}, \end{aligned} \tag{10}$$

where $i = \sqrt{-1}$; overbar means complex conjugate; superscript -1 means matrix inverse. Substitution of (9) into (1) gives the following Green's displacements:

$$U_{kl}^{*} = \frac{-1}{\pi} \operatorname{Re} \left[\sum_{j=1}^{3} A_{lj} D_{jk} \ln(z_j - z_j^0) \right] \tag{11}$$

and Green's tractions

$$T_{kl}^{*} = \frac{1}{\pi} \operatorname{Re} \left[\sum_{j=1}^{3} L_{lj} \frac{\mu_j n_x - n_y}{z_j - z_j^0} D_{jk} \right], \tag{12}$$

with n_x and n_y being the outward normal components of the field point.

3. The new boundary integral equations

The traditional displacement boundary integral equation is well-known, and can be expressed as

$$\begin{aligned} & c_{ij} u_j(\boldsymbol{Y}) + \fint_{\Gamma} T_{ij}^{*}(\boldsymbol{Y},\boldsymbol{X}) u_j(\boldsymbol{X})\, \mathrm{d}\Gamma(\boldsymbol{X}) \\ & \quad = \int_{\Gamma} U_{ij}^{*}(\boldsymbol{Y},\boldsymbol{X}) t_j(\boldsymbol{X})\, \mathrm{d}\Gamma(\boldsymbol{X}), \end{aligned} \tag{13}$$

where summation convention over repeated indexes is implied; U_{ij}^{*} and T_{ij}^{*} are the Green's displacements and tractions given in (11) and (12); u_j and t_j are boundary displacements and tractions; c_{ij} is a tensor whose elements depend on the geometry at point $\boldsymbol{Y}$; Γ is the boundary of the domain; and finally, a bar across the integral sign denotes the Cauchy singular integral. Discretization of (13) gives a linear system of algebraic equations which can be solved for the unknowns on the boundary. One important feature of (13) is that only a Cauchy type singularity is involved, which can be handled easily by the rigid-body motion method. For a cracked elastic medium as shown in Figure 1(a), however, (13) itself is not enough for solving all unknowns along the outer boundary as well as along the two sides of the crack surface because of the geometry singularity of the crack surface [16]. As mentioned before, the most efficient method for solving such a problem is the dual BEM [7, 8].

In the dual BEM method, the displacement boundary integral equation (13) is applied to the outside boundary Γ_B and to one side of the crack surface Γ_{C+}; the traction integral equation (14) below (assuming that $\boldsymbol{Y}$ is a smooth point on the boundary) is then applied to the other side of the crack surface Γ_{C-} (Figure 1(a))

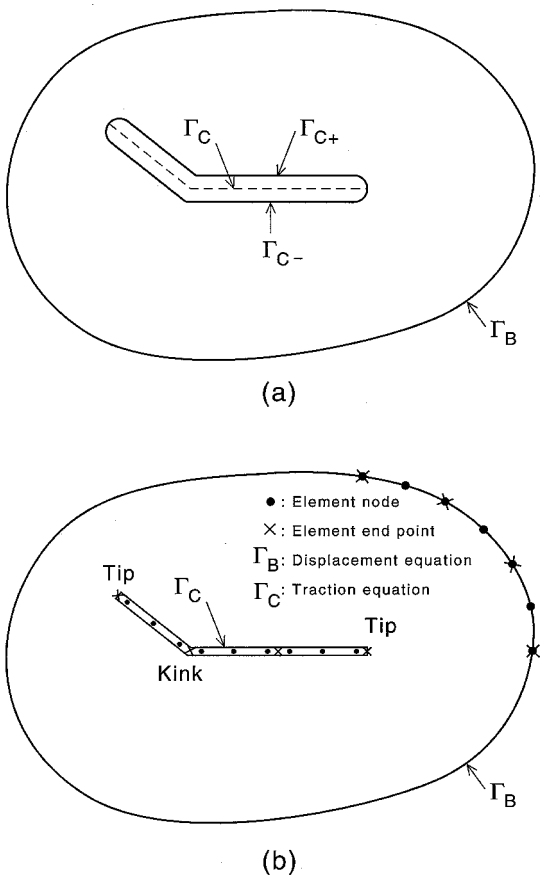

Figure 1. Geometry of a cracked 2-D anisotropic domain (a), and (b) its modelling with the quadratic boundary elements.

$$0.5t_l(\boldsymbol{Y}) + n_m(\boldsymbol{Y}) \,\text{=}\!\!\!\!\!\!\int_\Gamma c_{lmik}\, T^*_{ij,k}(\boldsymbol{Y},\boldsymbol{X}) u_j(\boldsymbol{X})\, \mathrm{d}\Gamma(\boldsymbol{X}) = n_m(\boldsymbol{Y}) \,\text{=}\!\!\!\!\!\!\int_\Gamma c_{lmik} U^*_{ij,k}(\boldsymbol{Y},\boldsymbol{X}) t_j(\boldsymbol{X})\, \mathrm{d}\Gamma(\boldsymbol{X}), \tag{14}$$

where n_m is the outward normal of the boundary or crack surface; c_{lmik} are the components of the stiffness tensor of the anisotropic medium; subscript prime followed by an index means derivative; and the double bars across the integral sign denotes a Hadamard finite-part integral [17]. This finite-part integral is very difficult to handle. Although different methods have been suggested to handle such an integral [18], they usually require the evaluation of a limit value of the integrand at the singular point, which is possible only for the case where the integrand has a simple and exact-closed form expression. If a medium is isotropic and if one assumes a piece-wise flat crack, the finite-part integral can then be carried out by a direct analytical integration [7, 8].

In this paper, we introduce a new BEM formulation for handling cracked anisotropic media. By contrast with the dual BEM for isotropic media, the new BEM does not require the double discretization on the crack surface, while it can be used to calculate the stress intensity factors as well as displacement and stress distributions in cracked isotropic and anisotropic

2-D media. The equations in the new BEM are formulated in such a way which possesses the advantages of both the traditional displacement BEM and the DDM.

In the new BEM formulation, we first apply the traditional displacement integral equation to the outside boundary *only*, which results in the following equation (see Figure 1(b)):

$$\begin{aligned} c_{ij}u_j(\boldsymbol{Y}_B) + \oint_{\Gamma_B} T^*_{ij}(\boldsymbol{Y}_B, \boldsymbol{X}_B)u_j(\boldsymbol{X}_B)\,\mathrm{d}\Gamma(\boldsymbol{X}_B) \\ + \int_{\Gamma_C} T^*_{ij}(\boldsymbol{Y}_B, \boldsymbol{X}_C)(u_j(\boldsymbol{X}_{C+}) - u_j(\boldsymbol{X}_{C-}))\,\mathrm{d}\Gamma(\boldsymbol{X}_C) \\ = \int_{\Gamma_B} U^*_{ij}(\boldsymbol{Y}_B, \boldsymbol{X}_B)t_j(\boldsymbol{X}_B)\,\mathrm{d}\Gamma(\boldsymbol{X}_B), \end{aligned} \tag{15}$$

where Γ_C has the same outward normal as Γ_{C+}; the subscript B and C denote the outside boundary and the crack surface, respectively (Figure 1). The kernel function T^*_{ij} in the second integral of (15), which is the Green's traction caused by the point forces, is the Green's displacement caused by the point displacement discontinuities [4, 19]. Since the above equation is undeterminate, we then apply the traction integral equation (for $\boldsymbol{Y}$ being a smooth point on the crack) to one side of the crack surface *only* (Figure 1(b)):

$$\begin{aligned} 0.5t_l(\boldsymbol{Y}_C) + n_m(\boldsymbol{Y}_C)\int_{\Gamma_B} c_{lmik}T^*_{ij,k}(\boldsymbol{Y}_C, \boldsymbol{X}_B)u_j(\boldsymbol{X}_B)\,\mathrm{d}\Gamma(\boldsymbol{X}_B) \\ + n_m(\boldsymbol{Y}_C)\oint_{\Gamma_C} c_{lmik}T^*_{ij,k}(\boldsymbol{Y}_C, \boldsymbol{X}_C)(u_j(\boldsymbol{X}_{C+}) - u_j(\boldsymbol{X}_{C-}))\,\mathrm{d}\Gamma(\boldsymbol{X}_C) \\ = n_m(\boldsymbol{Y}_C)\int_{\Gamma_B} c_{lmik}U^*_{ij,k}(\boldsymbol{Y}_C, \boldsymbol{X}_B)t_j(\boldsymbol{X}_B)\,\mathrm{d}\Gamma(\boldsymbol{X}_B), \end{aligned} \tag{16}$$

where the second integrand is the Green's traction caused by the point displacement discontinuities. In deriving (15) and (16), we have assumed that the tractions on both sides of the crack surface have the same magnitude but opposite sign.

Equations (15) and (16) are enough for solving the unknown displacements or tractions on the outside boundary ($\boldsymbol{Y}_B \in \Gamma_B$) and the unknown displacement differences on the crack surface ($\boldsymbol{Y}_C \in \Gamma_C \equiv \Gamma_{C+}$). This new formulation possesses the best attributes of the traditional displacement BEM (Cauchy type singularity only!) and the DDM (displacement jumps for crack modeling!). Since we have used the displacement differences, instead of the displacements themselves along the crack, as unknown, no double elements or nodes are required on the crack surface. It is also noted that because of the linearity, the superposition method can be applied to the above integral equations to handle infinite domain and gravity body-forces cases [20]. The remaining task is now the treatment of the singularities in (15) and (16) and the crack tip modeling.

4. Treatments of singular integrals and crack tips

The Cauchy type singularity in the displacement equation (15) can be avoided by the rigid-body motion method, which results in a row summation in the discretized form [20]. The integrand on the right-hand side of (15) has only integrable singularity, which can be handled easily by, for example, the bi-cubic transformation method [21].

The traction equation (16), however, involves a finite-part integral. As mentioned earlier, for isotropic materials with piece-wise flat crack assumption, the integral can be carried out by directly analytical integration [7, 8]. For anisotropic media, however, the integrand is very complicated and its analytical evaluation is impossible. Although the Taylor's series expansion method can be employed to regulate the singularity [7, 22], it requires some limit-value evaluations of the integrand which are possible only when the integrand has an exact-closed form expression.

In this paper, a weighted Gauss quadrature method [23] is employed to evaluate the finite-part integral accurately. This method is quite similar to the classical Gauss quadrature [24] and is very efficient. For the finite-part integral

$$I(f,s) = \oint_a^b \frac{w(x)f(x)}{(x-s)^2}\,\mathrm{d}x; \quad s \in (a,b), \tag{17}$$

we first construct a set of polynomials which are orthogonal with respect to $w(x)/(x-s)^2$, in which $w(x)$ is a non-negative weight function; From this set of polynomials, we then obtain the following accurate quadrature formula

$$I(f,s) = \sum_{j=1}^{n} g_{j,n}(s) f(x_j), \tag{18}$$

where $g_{j,n}(s)$ are the weights with respect to the singular point s, and x_j the corresponding coordinates.

On the crack surface, some continuity conditions are required [7, 8]. These conditions can be satisfied by using discontinuity quadratic elements [7, 8]. The node positions for these kinds of elements are $s = -\frac{2}{3}, 0, \frac{2}{3}$. For singularities at these three points, we construct the weights and coordinates $(w(x) \equiv 1)$ following Tsamasphyros and Dimou's procedure [23]. These weights and coordinates thus found have been tested for the following two finite-part integrals:

$$\oint_{-1}^{+1} \frac{\mathrm{d}x}{(x-s)^2} = \frac{-2}{1-s^2}, \tag{19}$$

$$\begin{aligned} &\oint_{-1}^{+1} \frac{(y^2-x^2)^{-1/2}\,\mathrm{d}x}{(x-s)^2} \quad (y^2 > 1) \\ &\quad = \frac{s}{(y^2-s^2)^{3/2}} \ln\left(\frac{(y^2-s^2)^{1/2} - s(y^2-1)^{1/2}}{(y^2-s^2)^{1/2} + s(y^2-1)^{1/2}}\right) - \frac{2(y^2-1)^{1/2}}{(y^2-s^2)(1-s^2)}. \end{aligned} \tag{20}$$

For both of these integrals, the absolute value of the difference between the exact, (19) and (20), and the approximate (numerical quadrature (18)) values is less than 10^{-11}.

In order to capture the square-root characteristics of the displacements near the crack tip, we constructed the following crack tip element with tip at $s = -1$

$$u_i = \sum_{k=1}^{3} \phi_k u_i^k, \tag{21}$$

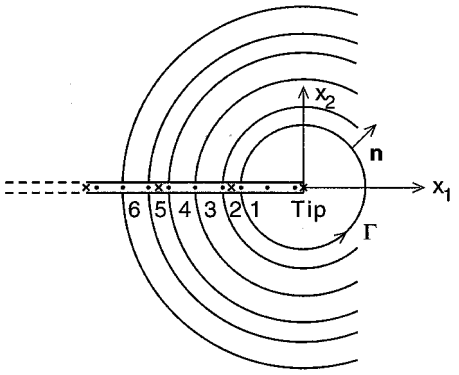

Figure 2. Different contour paths for J-integral.

where the subscript i denotes the components of the displacement and the superscript $k(=1,2,3)$ denotes the displacements at nodes $s=-\frac{2}{3},0,\frac{2}{3}$, respectively. The shape functions ϕ_k were found to be

$$\begin{aligned}
\phi_1 &= \left[\tfrac{5}{3}-\sqrt{\tfrac{5}{3}}-\tfrac{2}{3}\sqrt{s+1}+\left(\sqrt{\tfrac{5}{3}}-1\right)(s+1)\right]\Big/\Delta,\\
\phi_2 &= \left[\tfrac{1}{3}\sqrt{\tfrac{5}{3}}-\tfrac{5}{3}\sqrt{\tfrac{1}{3}}+\tfrac{4}{3}\sqrt{s+1}+\left(\sqrt{\tfrac{1}{3}}-\sqrt{\tfrac{5}{3}}\right)(s+1)\right]\Big/\Delta,\\
\phi_3 &= \left[\sqrt{\tfrac{1}{3}}-\tfrac{1}{3}-\tfrac{2}{3}\sqrt{s+1}+\left(1-\sqrt{\tfrac{1}{3}}\right)(s+1)\right]\Big/\Delta,\\
\Delta &= \tfrac{2}{3}\left(2-\sqrt{\tfrac{1}{3}}-\sqrt{\tfrac{5}{3}}\right).
\end{aligned} \tag{22}$$

5. Calculation of stress intensity factor

Previously, different techniques within the BEM scope, such as near-tip displacement extrapolation, near-tip stress extrapolation [25], and J-integral [7, 8, 26] methods, have been proposed to calculate the stress intensity factors. Among these methods, the J-integral method is the most accurate one [7, 8]. This method can be easily applied to either mode I or mode II crack problem. However, it can not be directly applied to mixed mode problems. Recently, Sollero and Aliabadi [2] proposed a decoupling procedure for calculating the mixed-mode stress intensity factors. This approach is simple and accurate, and can be presented as follows.

The definition of the J_k integral is [2, 27]

$$J_k=\int_\Gamma \sum_{i,j=1}^{2}\left(\tfrac{1}{2}\sigma_{ij}e_{ij}n_k-\sigma_{ji}n_iu_{j,k}\right)\,\mathrm{d}\Gamma \quad (k=1,2), \tag{23}$$

where Γ is a generic contour surrounding the crack tip (Figure 2); σ_{ij} and e_{ij} are the stress and strain tensors respectively, and n_i are the unit outward normal to the contour path.

It can be shown [27] that for a cracked 2-D homogeneous and anisotropic medium free of body forces, the above J_k integral is related to the stress intensity factors by

$$\begin{aligned} J_1 &= \alpha_{11} K_{\mathrm{I}}^2 + \alpha_{12} K_{\mathrm{I}} K_{\mathrm{II}} + \alpha_{22} K_{\mathrm{II}}^2, \\ J_2 &= \gamma_{11} K_{\mathrm{I}}^2 + \gamma_{12} K_{\mathrm{I}} K_{\mathrm{II}} + \gamma_{22} K_{\mathrm{II}}^2, \end{aligned} \tag{24}$$

where α_{ij} and γ_{ij} are constants related to the elastic properties of the anisotropic medium [2, 27]. Assuming the crack is traction free, we note from (23) that along the crack surfaces, the J_1 integral vanishes whereas the J_2 integral involves a highly singular integrand. In order to avoid this difficulty, we follow Sollero and Aliabadi's decoupling method [2]. By expanding the displacements near the crack tip, we find that the ratio of the displacement differences near the crack tip is (Figure 2)

$$R \equiv \frac{u_2^+ - u_2^-}{u_1^+ - u_1^-} = \frac{H_{21} K_{\mathrm{I}} + H_{22} K_{\mathrm{II}}}{H_{11} K_{\mathrm{I}} + H_{12} K_{II}}, \tag{25}$$

where

$$\begin{aligned} H_{11} &= \mathrm{Im}\left(\frac{\mu_2 A_{11} - \mu_1 A_{12}}{\mu_1 - \mu_2}\right); \qquad H_{12} = \mathrm{Im}\left(\frac{A_{11} - A_{12}}{\mu_1 - \mu_2}\right); \\ H_{21} &= \mathrm{Im}\left(\frac{\mu_2 A_{21} - \mu_1 A_{22}}{\mu_1 - \mu_2}\right); \qquad H_{22} = \mathrm{Im}\left(\frac{A_{21} - A_{22}}{\mu_1 - \mu_2}\right). \end{aligned} \tag{26}$$

Solving (25), we find the ratio of stress intensity factors as

$$\frac{K_{\mathrm{I}}}{K_{\mathrm{II}}} = \frac{R H_{12} - H_{22}}{H_{21} - R H_{11}} \equiv F. \tag{27}$$

Substituting (27) into (24), and solving for K_{II} gives the following equation

$$K_{\mathrm{II}} = \sqrt{\frac{J_1}{\alpha_{11} F^2 + \alpha_{12} F + \alpha_{22}}}. \tag{28}$$

Once K_{II} is obtained from (28), K_{I} then follows from (27).

6. Numerical examples

Three illustrative examples were selected to test our new BEM formulation. The latter was implemented into a BEM program written by the authors. All examples assume plane stress. The first example corresponds to a finite crack $(a = 0.25)$ in an infinite medium under a uniform far-field stress σ in the y-direction (Figure 3). The material is isotropic with a Young's modulus $E = 4$ (in dimensionless) and a Poisson's ratio $\nu = 0.25$ (Since the Green's functions in (11) and (12) are singular in the isotropic limit, a small difference of the Young's moduli in the x_1 and x_2 directions is given [3]). For this infinite problem with a single crack, we need (16) only. The crack surface was discretized using 10 discontinuous quadratic elements. The crack opening displacements (in dimensionless) $\Delta u_y = u_y(x, 0+) - u_y(x, 0-)$ are given in Table 1. In this table, the second and third columns are the results obtained with the new BEM formulation assuming no crack tip elements (method I) and crack tip elements given

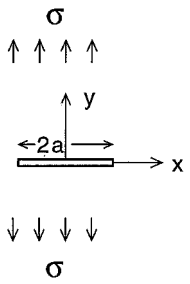

Figure 3. A finite crack in an infinite and isotropic medium under a uniform far-field stress in y-direction.

Table 1. Crack opening displacements for a single crack in an infinite and isotropic medium

X	Δu_y (Method I)	Δu_y (Method II)	Δu_y (Exact)
0.241667E+00	0.743954E−01	0.639519E−01	0.640096E−01
0.225000E+00	0.113923E+00	0.108657E+00	0.108972E+00
0.208333E+00	0.141119E+00	0.138338E+00	0.138193E+00
0.191667E+00	0.163109E+00	0.160783E+00	0.160511E+00
0.175000E+00	0.180967E+00	0.178633E+00	0.178536E+00
0.158333E+00	0.195693E+00	0.193459E+00	0.193470E+00
0.141667E+00	0.208148E+00	0.206001E+00	0.205987E+00
0.125000E+00	0.218586E+00	0.216510E+00	0.216506E+00
0.108333E+00	0.227308E+00	0.225294E+00	0.225308E+00
0.916667E−01	0.234553E+00	0.232589E+00	0.232588E+00
0.750000E−01	0.240409E+00	0.238485E+00	0.238485E+00
0.583333E−01	0.244987E+00	0.243093E+00	0.243099E+00
0.416667E−01	0.248376E+00	0.246504E+00	0.246503E+00
0.250000E−01	0.250606E+00	0.248748E+00	0.248747E+00
0.833333E−02	0.251710E+00	0.249860E+00	0.249861E+00

by (21) and (22) (method II). The last column is the exact solution [28]. It is noted from this table that introduction of the crack tip elements greatly improves the results. This conclusion can be further verified by calculating the corresponding stress intensity factors.

For the example of Figure 3, the exact normalized stress intensity factor, $K_{\mathrm{I}}/\sigma\sqrt{(\pi a)}$ is 1. Numerically, we calculated this stress intensity factor by the J-integral method with different circles as shown in Figure 2. For all these calculations, the circle was divided into four quarters and a 6 points open-type Newton-Cotes formula [29] was applied to each quarter. Again, the results in Table 2 show clearly that addition of the crack tip elements dramatically improves the accuracy.

The second example is a kinked crack in an isotropic and infinite medium under a uniform far-field stress in the y-direction (Figure 4). As for the first example, we need (16) only. Since this is a mixed mode problem, the decoupling technique [2] needs to be used, (27) and (28). In this example, the inclined crack branch $(b = 0.2a)$ is inclined at 45 degrees to the horizontal direction. We used 6 and 10 discontinuous quadratic elements for the inclined branch and horizontal crack section, respectively. The normalized stress intensity factors at tips A and B are presented in Table 3 along with the results from Mews [30], Sih [31] and Murakami [32].

Table 2. Normalized stress intensity factors for a single crack in an infinite and isotropic medium

Circle	$K_{\rm I}/\sigma\sqrt{(\pi a)}$ (Method I)	$K_{\rm I}/\sigma\sqrt{(\pi a)}$ (Method II)
1	0.9767	1.000406
2	0.9750	0.999461
3	0.9744	0.999792
4	0.9746	1.000005
5	0.9752	0.999995
6	0.9756	1.000003

Clearly, very accurate results are obtained with the authors' program based on the new BEM formulation.

As a third and final example, an anisotropic, and finite rectangular plate with a central crack inclined at 45 degrees to the horizontal direction is considered (Figure 5). The plate is under uniform tension in the y-direction. The ratios of crack length to width, and of height to width are $a/w = 0.2$ and $h/w = 2.0$, respectively. The material is of glass-epoxy with properties $E_1 = 48.26\,\text{GPa}$, $E_2 = 17.24\,\text{GPa}$, $\nu_{12} = 0.29$, and $G_{12} = 6.89\,\text{GPa}$ [2]. The direction of the fibers was rotated from $\Psi = 0$ to $\Psi = 180$ degrees. The two normalized stress intensity factors were calculated with the present BEM program using 10 discontinuous quadratic elements on the crack surface and 32 quadratic elements on the outside boundaries. Table 4 shows the results obtained by the authors' new BEM formulation as well as those by Gandhi [33] with a mapping-collocation technique, and by Sollero and Aliabadi [2] with a subregional BEM. Again, excellent agreement is obtained.

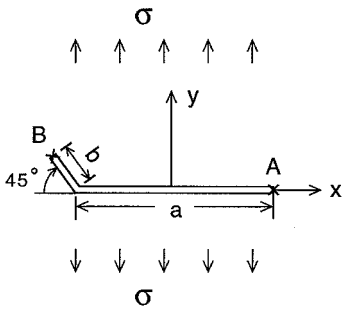

Figure 4. A kinked finite crack in an infinite and isotropic medium under a uniform far-field stress in y-direction.

Table 3. Normalized stress intensity factors for a kinked crack in an infinite and isotropic medium

	$K_{\rm I}^A/\sigma\sqrt{(\pi a)}$	$K_{\rm II}^A/\sigma\sqrt{(\pi a)}$	$K_{\rm I}^B/\sigma\sqrt{(\pi a)}$	$-K_{\rm II}^B/\sigma\sqrt{(\pi a)}$
Mews [30]	0.7512	0.0204	0.4479	0.4213
Sih [31]	0.7522	0.0212	0.4513	0.4223
Murakami [32]	0.7517	0.0212	0.4520	0.4214
Present	0.7520	0.0213	0.4523	0.4233

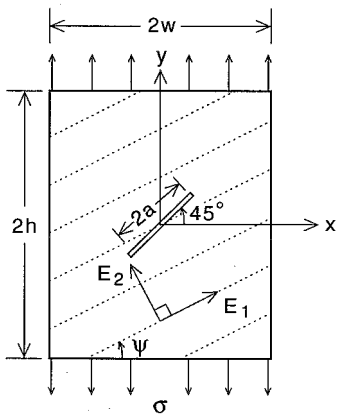

Figure 5. An anisotropic and finite rectangular plate with a central crack inclined 45 degrees to horizontal direction under a uniform tension in y-direction.

Table 4. Normalized stress intensity factors for a central inclined crack in an anisotropic and finite rectangular plate

	$K_{\mathrm{I}}/\sigma\sqrt{(\pi a)}$			$K_{\mathrm{II}}/\sigma\sqrt{(\pi a)}$		
Ψ	Sollero and Aliabadi [2]	Present	Gandhi [33]	Sollero and Aliabadi [2]	Present	Gandhi [33]
0	0.510	0.519	0.522	0.500	0.504	0.507
45	0.512	0.516	0.515	0.508	0.505	0.505
90	0.525	0.537	0.513	0.507	0.532	0.509
105	0.527	0.507	0.517	0.504	0.502	0.510
120	0.525	0.520	0.524	0.502	0.508	0.512
135	0.519	0.532	0.532	0.504	0.511	0.511
180	0.510	0.519	0.522	0.500	0.504	0.507

7. Conclusions

A new BEM formulation has been proposed for fracture mechanics analysis of cracked 2-D anisotropic elastic media. In this new approach, the displacement and traction integral equations are collocated on the outside boundary (no-crack boundary) only and on one side of the crack surface only, respectively. Therefore, no double elements and nodes are required along the crack surface. Furthermore, since the new BEM formulation uses displacements or tractions as unknowns on the outside boundary and displacement differences as unknowns along the crack surface, it combines the best attributes of the traditional displacement BEM and the DDM. While the Cauchy singularity in the displacement equation is avoided by the common rigid-body motion method, the hyper-singularity in the traction equation is handled by introducing a new Gauss quadrature formulae which is very similar to the traditional weighted Gauss quadrature but with a different weight. To calculate the mixed mode stress intensity factors, the authors employ the decoupling technique developed in [2]. A new set of crack tip elements is also introduced, which can dramatically improve the accuracy of the stress intensity factors.

The new BEM program can handle 2-D anisotropic, finite as well as infinite domain problems with any kind of crack geometry. To verify the new program, three examples including infinite as well as finite domains, isotropic as well as anisotropic media, straight as well as kinked crack geometry shapes were run. All these examples show excellent agreement with previously published results in the literature. Since the present method is simple, and can also be used for curved cracks, it will be straightforward to extend the new BEM formulation to analyze fracture propagation in 2-D anisotropic media. This is currently under investigation by the authors, and the results will be reported in a separate paper.

Acknowledgements

Mr. Chao-Shi Chen ran some of the numerical examples for us. This research is funded by National Science Foundation, Grant No. MS-9215397.

References

1. M.D. Snyder and T.A. Cruse, *International Journal of Fracture* 11 (1975) 315–328.
2. P. Sollero and M.H. Aliabadi, *International Journal of Fracture* 64 (1993) 269–284.
3. P. Sollero, M.H. Aliabadi and D.P. Rooke, *Engineering Fracture Mechanics* 49 (1994) 213–224.
4. S.L. Crouch and A.M. Starfield, *Boundary Element Methods in Solid Mechanics*, George Allen and Unwin Publishers, London (1983).
5. H.K. Hong and J.T. Chen, *Journal of Engineering Mechanics* 114 (1988) 1028–1044.
6. L.J. Gray, L.F. Martha and A.R. Ingraffea, *International Journal for Numerical Methods in Engineering* 29 (1990) 1135–1158.
7. A. Portela, M.H. Aliabadi and D.P. Rooke, *International Journal for Numerical Methods in Engineering* 33 (1992) 1269–1287.
8. S. Guimaraes and J.C.F. Telles, *Engineering Analysis with Boundary Elements* 13 (1994) 353–363.
9. N.N.V. Prasad, M.H. Aliabadi and D.P. Rooke, *International Journal of Fracture* 66 (1994) 255–272.
10. Ibid, R45-R50.
11. S.G. Lekhnitskii, *Theory of Elasticity of an Anisotropic Body*, Holden Day, San Francisco (1963).
12. J.D. Eshelby, W.T. Read and W. Shockley, *Acta Metallurgica* 1 (1953) 251–259.
13. A.N. Stroh, *The Philosophical Magazine* 7 (1958) 625–646.
14. Z. Suo, *Proceedings of the Royal Society* (London), A427 (1990) 331–358.
15. E. Pan and B. Amadei, *Journal of Engineering Mechanics* 120 (1994) 97–119.
16. T.A. Cruse, in *Developments in Boundary Element Methods* – P.K. Banerjee and R. Butterfield (eds.), Applied Science Publishers Ltd., London (1979).
17. D.F. Paget, *Numerische Mathematik* 36 (1981) 447–453.
18. A.M. Linkov, *Acta Mechanica* 105 (1994) 189–205.
19. E. Pan, *Acta Mechanica* 87 (1991) 105–115.
20. E. Pan and B. Amadei, *Applied Mathematical Modelling* 20 (1996) 114–120.
21. M. Cerrolaza and E. Alarcon, *International Journal for Numerical Methods in Engineering* 28 (1989) 987–999.
22. J. Hildenbrand and G. Kuhn, *International Journal for Numerical Methods in Engineering* 36 (1993) 2939–2954.
23. G. Tsamasphyros and G. Dimou, *International Journal for Numerical Methods in Engineering* 30 (1990) 13–26.
24. A.H. Stroud and D. Secrest, *Gaussian Quadrature Formulas*, Prentice-Hall, Inc., Englewood Cliffs, N.J. (1966).
25. Y. Sato, M. Tanaka and M. Nakamura, *Engineering Analysis with Boundary Elements* 1 (1984) 200–205.
26. J.R. Rice, *Journal of Applied Mechanics* 35 (1968) 379–386.
27. S.J. Chu and C.S. Hong, *Engineering Fracture Mechanics* 35 (1990) 1093–1103.
28. M.H. Aliabadi and D.P. Rooke, *Numerical Fracture Mechanics*, Computational Mechanics Publications, Southampton, and Kluwer Academic Publishers, Dordrecht (1991).
29. M. Abramowitz and I.A. Stegun, *Handbook of Mathematical Functions*, Dover Publications, Inc., New York (1972).
30. H. Mews, *Proceedings of the 9th International Conference on Boundary Element Method*, C.A. Brebbia, W.L. Wendland and G. Kuhn (eds.), 2 (1987) 259–278.

31. G.C. Sih, *Handbook of Stress-Intensity Factors*, Lehigh University, Bethlehem, Pennsylvania (1973).
32. Y. Murakami, *Stress Intensity Factors Handbook*, Pergamon Press, Oxford (1987).
33. K.R. Gandhi, *Journal of Strain Analysis* 7 (1972) 157–162.